Healing of the Palatal Removal Sites after Removal of Miniscrew-Assisted Rapid Palatal Expansion

Nguyen, Hieu

Department of Dentistry

Graduate School

Yonsei University

Healing of the Palatal Removal Sites after Removal of Miniscrew-Assisted Rapid Palatal Expansion

Advisor: Choi, Yoon Jeong

A Dissertation Submitted
to the Department of Dentistry
and the Committee on Graduate School of Yonsei University
in Partial Fulfillment of the
Requirements for the Degree of
Doctor of Philosophy in Dental Science

Nguyen, Hieu

June 2025

Healing of the Palatal Removal Sites after Removal of Miniscrew-Assisted Rapid Palatal Expansion

This Certifies that the Dissertation of Nguyen, Hieu is approved

Committee Chair: Lee, Kee-Joon

Committee Member: Choi, Yoon Jeong

Committee Member: Lee, Hyeonjong

Committee Member: Lee, Chena

Committee Member: Kim, Dong-Jae

Department of Dentistry

Graduate School

Yonsei University

June 2025

ACKNOWLEDGE

In all sincerity, I would like to express my gratitude to the following people who encouraged and supported me to complete this Doctor of Philosophy's degree. Time in Yonsei University with all of them will be one of the most wonderful experiences and unforgettable in my life.

First and foremost, I extend my heartfelt appreciation to my thesis advisor, Professor. Choi, Yoon Jeong to guide me throughout the research work. Her immense knowledge, exceptional mentorship, invaluable insights, and boundless patience have given me more motivation during the research process. Her dedication to excellence and her commitment to pushing the boundaries of knowledge have been instrumental in shaping this work.

Apart from my Supervisor, I am profoundly grateful to the members of my thesis committee, Professor. Lee, Kee-Joon, Professor. Lee, Hyeonjong, Professor. Lee, Chena, and Professor. Kim, Dong-Jae, for their expertise, valuable feedback, and constructive suggestions, which have greatly enriched the quality of this research.

I would like to thank my colleagues at the Department of Orthodontics, Yonsei University College of Dentistry. Your support and camaraderie have made this academic journey not only productive but also enjoyable.

Lastly, my heartfelt thanks go to my wife, my daughter, my family, and my friends for their unwavering encouragement, understanding, and patience during this challenging journey.

TABLE OF CONTENTS

LIST OF FIGURES

LIST OF TABLES

ABBREVIATIONS

Miniscrew-assisted rapid palatal expansion	MARPE
Cone beam computed tomography	CBCT
Midpalatal suture	MPS
Digital imaging and communications in medicine	DICOM
Standard tessellation language	STL
Palatal bone thickness	PBT
Volume healing ratio	VHR
Total surface area healing ratio	TSAHR
Intraclass correlation coefficient	ICC

ABSTRACT

Healing of Palatal Removal Sites after Removal of Miniscrew-Assisted Rapid Palatal Expansion

Nguyen Hieu, D.D.S, M.S.D.,

Department of Dentistry

The Graduate School, Yonsei University

(Directed by Professor Choi Yoon Jeong, D.D.S., M.S.D, Ph.D.)

This study aimed to evaluated healing of the palatal bone healing after miniscrew removal in patients treated by with a miniscrew-assisted rapid palatal expander (MARPE) and identified key factors influencing the healing process.

This retrospective study included 152 removal sites(76 anterior and 76 posterior sites) from 38 adult patients who underwent MARPE treatment. To investigate the healing of the palatal removal sites, the following measurement were performed: miniscrew inclination, distance to the midpalatal suture (MPS), palatal bone thickness (PBT), and widths, depth, volume, total surface area of the removal sites at the end of the consolidation phase (T1) and over six months post-removal (T2). Additionally, volume healing ratio (VHR) and total

surface area healing ratio (TSAHR) were compared between anterior and posterior removal sites, as well as between mono-cortical and bicortical anchorages. Correlation between healing ratios and patient demographic or clinical factors were analyzed.

After removal of miniscrew, all dimension, volume, and total surface area of the removal sites decreased significantly ($P < 0.05$). VHR of anterior removal sites (98.3 ± 1.1%) was significantly higher than that of posterior sites (86.6 ± 9.7%) ($P < 0.001$). Mono-cortical anchorage sites (96.5 ± 4.6%) healed significantly better than bicortical anchorage sites (84.4 ± 10.2%) ($P < 0.001$). Healing ratio at the posterior removal sites was significantly correlated with age at T2, time duration, MARPE expansion width, distance to MPS, and cortical anchorage type ($P < 0.05$).

Substantial recovery was shown at the palatal bone removal sites after MARPE, closely resembling pre-treatment conditions. Superior healing was observed in anterior regions and mono-cortical anchorage sites, while healing at posterior sites was influenced by patient demographics and miniscrew characteristics.

Keywords: MARPE, palatal bone, bone healing, miniscrew

I. INTRODUCTION

In literature, from 8.0 to 23.3% of patients in children and teenagers, and 9.4% patients in adults has been reported to have maxillary constriction (Brunelle et al., 1996). To resolve the maxillary transverse discrepancy, separation of the midpalatal suture (MPS) has been considered to be an effective treatment (Haas, 1961). Due to the increase of bony resistance of the maxillary complex in adult, miniscrew-assisted rapid palatal expansion (MARPE) has been developed as an effective substitution to conventional rapid palatal expansion (Lee et al., 2010). Four miniscrews to separate the maxillary bone in MARPE need to be removed after the completion of MPS expansion.

Bone healing after miniscrew removal has been rarely evaluated although there have been numbers of studies to investigate the effectiveness of miniscrew in orthodontic treatment. Clinically, miniscrew removal is not considered a invasive procedure, and the intraoral wounds after removal are expected to undergo spontaneous healing (Jung et al., 2015; Kravitz et al., 2007). Nevertheless, a moderate risk of irreversible scarring on the soft tissue and disturbed wound healing due to bony sequestrum has been revealed at the removal site (Jung et al., 2015; Choi et al., 2015; Fäh et al., 2014). Another *in vivo* study suggested that the quality and anatomy of the alveolar bone at the removal site took longer time to reach similar levels to that of surrounding bone, although quantitative bone healing was observed after miniscrews removal (Kim et al., 2019).

Miniscrews included in MARPE may show different pattern of healing after removal from those used for routine orthodontic force. The miniscrews in MARPE used for MPS separation and orthopedic expansion should endure significantly higher force, up to 150 N, at the apex of the palate compared to those implanted into the interradicular bone (Walter

et al., 2023; MacGinnis et al., 2014). With MARPE, the maximum stress (about 560 g/mm^2) was confirmed to be concentrated around the miniscrews (Seong et al., 2018). Furthermore, a recent study reported an incomplete healing of the MPS 16 months after expansion, and the most commonly unrepaired region is the middle third of the palate, compared to the anterior and posterior regions of the hard palate (Naveda et al., 2022). This raises concerns about possibility of insufficient palatal bone healing after miniscrew removal, in patients treated by MARPE.

Even though MARPE was introduced over a decade ago and has gained significant attention from researchers and clinicians, detailed information on the healing of the palatal bone after miniscrew removal is still lacking in the literature (Lee et al., 2010). Therefore, this study aimed to investigate healing of the palatal removal sites after miniscrew removal in patients treated by MARPE using cone beam computed tomography (CBCT) images. In conducting this study, the null hypothesis that there is no healing at the palatal removal site after miniscrew removal was tested. Additionally, the study examine whether a relationship exists between the healing ratio of the removal site and demographic features of the patients, as well as the characteristics of the miniscrew.

II. MATERIAL AND METHODS

1. Samples

This retrospective study involved patients who underwent MARPE treatment between 2013 and 2023 at the Department of Orthodontics, Yonsei University Dental Hospital. The study protocol complied with the Declaration of Helsinki and was approved by the Institutional Review Board of Yonsei University Dental Hospital (IRB No 2-2024-0062). The requirement of written informed consent was waived because of the retrospective nature of this study.

The inclusion criteria were as follows: age between 16 and 40 years; availability of CBCT images taken both at the end of the consolidation phase before miniscrew removal (T1) and more than 6 months after miniscrew removal (T2); absence of craniofacial deformity and systematic diseases; and no previous orthodontic treatment. Additionally, the exclusion criteria included CBCT images with X-ray, patients, or scanner-related artifacts, as well as image noise; unavailability of CBCT images at either T1 or T2; miniscrew failure during expansion, and MPS expansion failure (Figure 1) (Nagarajappa et al., 2015).

Based on a previous study, the minimal sample size required to investigate the healing of palatal removal sites was calculated to be at least 62 sites (Kim et al., 2019). This was determined using the G-power program (G* Power 3.1.9.4, Dusseldorf, Germany) with a significance level of 0.05, power of 80%, and an effect size of 0.7.

CBCT images used in this study had been captured previously during orthodontic treatment to confirm suture separation, monitor expansion patterns, and assess periodontal status. The imaging conditions were set at 80 kV, 10.0 mA, field of view (FOV) of 150 x

150 mm^2, a scan time of 17 seconds, and a voxel size of 0.3 mm (Alphard-3030; ASAHI Roentgen IND, Kyoto, Japan). During image capturing, patients were guided to seat upright with Frankfort horizontal plane parallel to the floor. The patient's head was stabilized by an ear rod. For standardization across all subjects, all CBCT data sets included in this study met these exact specifications and were obtained using the same CBCT device.

The MARPE appliance (Kee's Bone Expander, Biomaterials Korea, Seoul, Korea) was used with banding of the maxillary first molars and first premolars. The MARPE appliance was installed with four self-drilled miniscrews incorporated into the palatal bone connected to the jackscrew. Two miniscrews were inserted in the anterior rugae region, while two were inserted in the posterior sagittal area. The miniscrews used were from two brands (Orlus, Ortholution, Seoul, Korea; and BMK, Biomaterials Korea, Seoul, Korea) and ranged 1.5–2.0 mm in diameter and 6.0–13.0 mm in length (Table 2). The activation of MARPE appliance was set at one turn per day (0.2 mm/ turn). Once the separation of the MPS was confirmed after 14 days, continuous expansion was performed until the palatal cusp of the maxillary first molars came into contact with the buccal cusp of the mandibular first molars. The consolidation period was 3-6 months after expansion phase. If the separation of MPS was not confirmed, the following protocol was performed: the expansion was discontinued for 4 weeks, followed by an additional expansion of 14 days. If the MPS was still not open after 14 days, the expansion was discontinued (Jeon et al., 2022; Lee et al., 2022). Age at T2, sex, and the duration between T1 and T2 were noted from the dental record. The total amount of MARPE expansion was calculated by the number of activations noted in the record (Table 1).

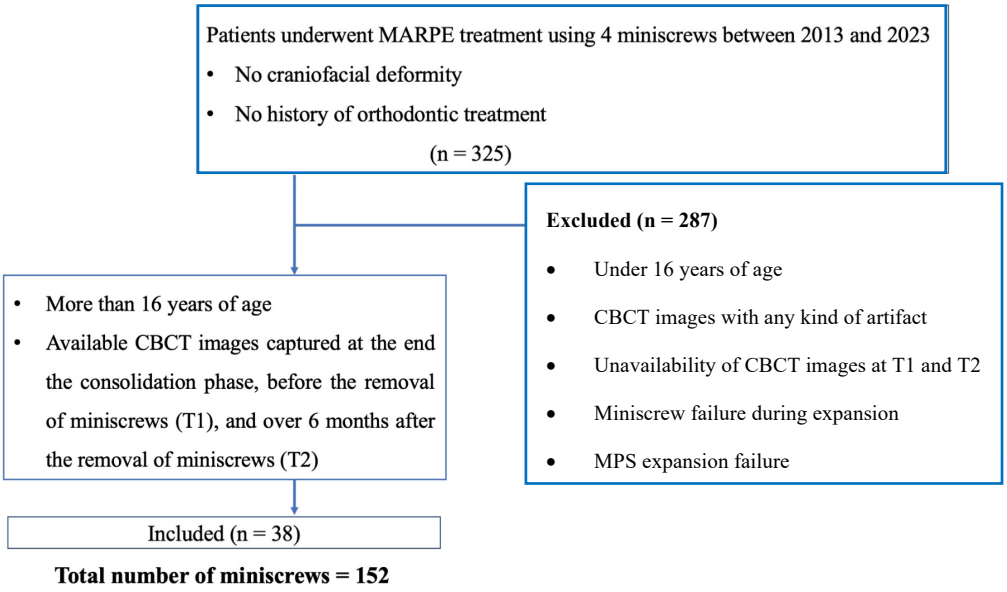

Figure 1. Flow chart of the sample enrollment

2. Measurements

2.1. Reorientation of T1 and T2 CBCT images

For the reorientation, CBCT images at T1 and T2 were captured and storaged as digital imaging and communications in medicine (DICOM) files with anonymization, which were imported to ITK-SNAP software (version 4.2.0; www.itksnap.org, Penn Image Computing and Science Laboratory, Philadelphia, PA, USA) and OnDemand3D software (CyberMed Inc., Seoul, Korea) as illustrated in Figure 2.

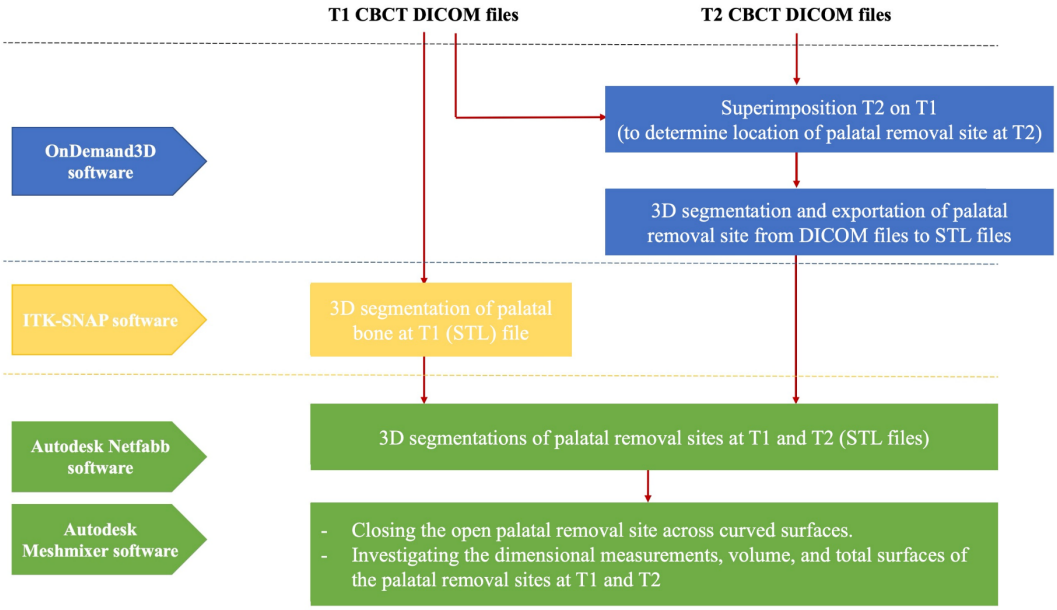

Figure 2. Flow chart of investigation method to identify the palatal removal sites

Then, the three axes coordinate system (x, y, and z) with the origin located at nasion point were used for the reorientation of CBCT files. Transverse axis (x-axis) was parallel to the orbital line. Anteroposterior axis (y-axis) was parallel to the right Frankfort line and perpendicular to the orbital line. Vertical axis (z-axis) was perpendicular to both the anteroposterior and transverse axes (Figure 3).

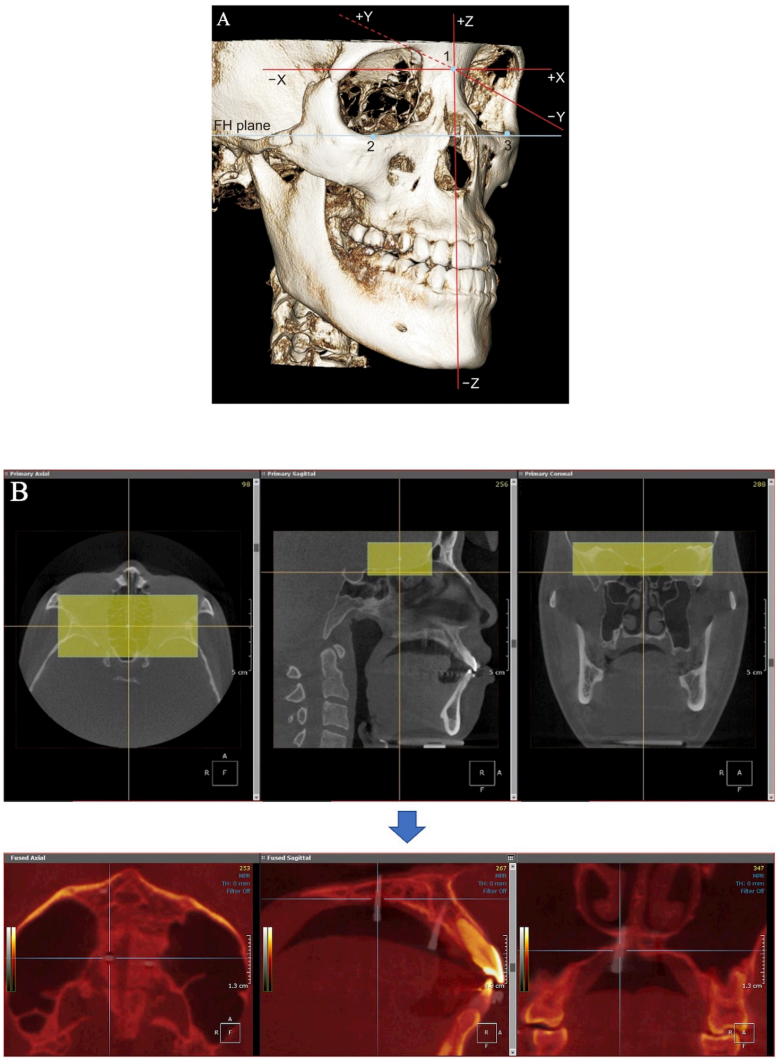

Figure 3. Reorientation and superimposition process of the CBCT images. A, reorientation of the three-dimensional images at T1 and T2; B, superimposition of CBCT at T2 onto T1 to determine the location of miniscrews at T2. 1, nasion; 2, orbitale right; 3, orbitale left; FH plane, Frankfort plane. The yellow boxes indicate the superimposition area at the cranial base.

2.2. Identifying palatal removal site created by miniscrew at T1

To identify the region of interest (ROI) at T1, the T1 DICOM files were exported to ITK-SNAP software (version 4.2.0; www.itksnap.org, Penn Image Computing and Science Laboratory, Philadelphia, PA, USA). The palatal bone was identified as the region of interest (ROI) for a semi-automatic segmentation process, consisting of a two-stage pipeline: an intensity-based pre-segmentation stage followed by an active contour segmentation stage (Yushkevich et al., 2006). (Figure 4). In the pre-segmentation stage, thresholding mode was used to transform the input greyscale image into a binary blue-to-white color map, distinguishing the palatal bone region (foreground) from non-palatal bone regions (background). This pre-segmentation was based on global thresholding, which requires a selection of thresholds to set the intensity bounds from the foreground (Colebank et al., 2019). A contrast calibration was established based on image intensity, with the lower threshold set at 260 gray level and the upper threshold at 2224 gray level (Friedli et al., 2020; Lee et al., 2014). In the active contour segmentation stage, seed points were manually placed within the ROI. The region- growing algorithm then selected all voxels connected to the initial seed based on a similar grayscale intensity range. Each selected voxel became a new seed, allowing the algorithm to iteratively refine the boundary of the palatal bone until the growth process stopped. Neighboring voxels with similar properties were merged to form closed regions (Yushkevich et al., 2019). This semi-automatic segmentation method has been shown to be more accurate, reliable, and faster than manual segmentation (Gomes et al., 2020). Due to the difference in grey intensity threshold values between the palatal bone and the miniscrew material, the area occupied by the miniscrew at T1 was visualized and segmented to stereolithography (STL) files (Figure 4).

2.3. Identifying palatal removal sites after removal of MARPE at T2

T2 ROI was identified based on the location of miniscrews at T1. The superimposition process was performed based on the anterior cranial base, which was introduced in previous report (Cevidanes et al., 2009). The superimposition method used voxel grayscale and was fully automated process by the software to avoid operator-related errors. This method has been validated for accuracy (Bazina et al., 2018). Once the superimposition was completed, the palatal bony defect at T2 was identified and exported to standard tessellation language (STL) files, with the highest resolution (Figure 5).

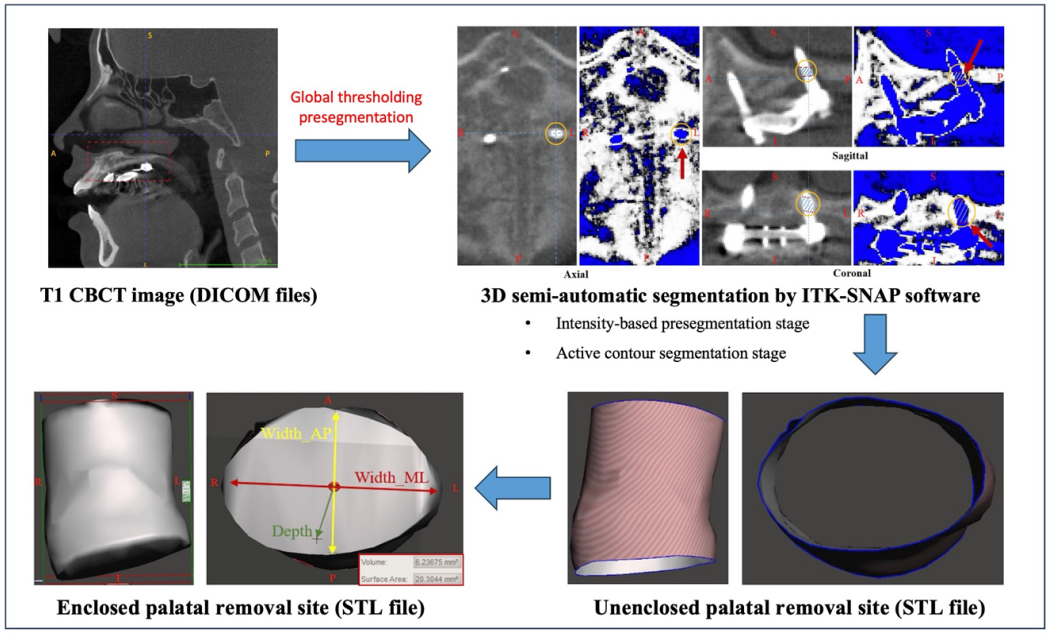

Figure 4. Three-dimensional segmentation and reconstruction of the palatal removal site created by miniscrew at T1. A, anterior; P, posterior; S, superior; I, inferior; R, right; L, left; T1, CBCT taken at the end of the consolidation phase, just before miniscrew removal; The yellow circles indicate the miniscrew portion within the bone at T1.

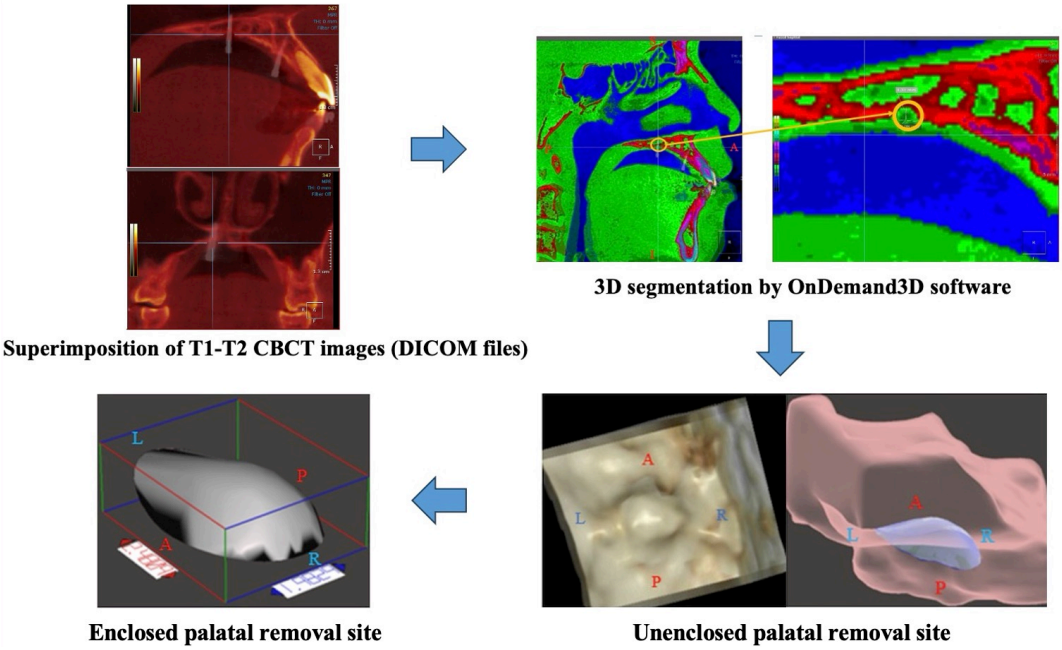

Figure 5. Three-dimensional segmentation and reconstruction of the palatal defect after miniscrew removal at T2. A, anterior; P, posterior; I, inferior; R, right; L, left; T2, CBCT taken over 6 months after miniscrew removal; The yellow circles indicate the palatal bony defects after miniscrew removal at T2.

2.4. Measurements

The measurements were conducted by a well-trained single examiner with 5 years of experience of CBCT investigation.

The unenclosed STL files of the T1 and T2 palatal removal sites were imported to Autodesk Netfabb and Autodesk Meshmixer softwares (Autodesk, San Rafael, CA, USA) to reconstruct the palatal removal sites across curved surfaces (de Freitas et al., 2023). The semi-automatic closing procedure was performed by inserting new triangles along open triangle edges, to make a mesh watertight (Charton et al., 2020). As the palatal removal site are non-trivial holes which are enclosed by more than three triangles, the circumference

needs to be traversed and triangles be added to close it. The surface sampling method or closing mesh across curved surfaces was selected to the surrounding triangle's orientation to regenerate the original shape (Li., 1995).

On the coronal section of the reconstructed T1 images, the inclination of the miniscrew axis, defined as the angle measured by connecting the long axis of the miniscrew to the perpendicular line of the palatal plane in mediolateral direction; on the axial section, the distance from the miniscrew to the MPS, measured from the center of the miniscrew to the hemi-section of the MPS after expansion; and on the sagittal section, the palatal bone thickness (PBT) at the miniscrew insertion site was measured (Table 1; Figure 6).

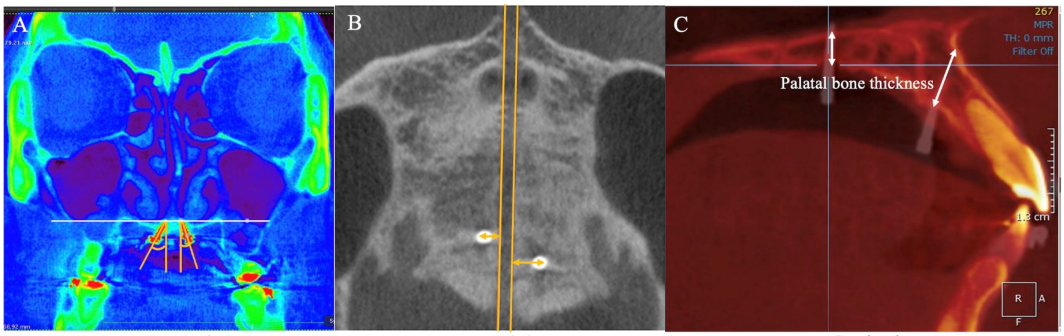

Figure 6. Miniscrew position measurements at T1. A, inclination angle between miniscrew axis and the perpendicular line to the palatal plane in mediolateral direction; B, perpendicular distance of miniscrew to the midpalatal suture; C, palatal bone thickness at the miniscrew insertion site at T1.

To quantify the palatal removal sites, dimensional measurements at T1 and T2—including width, depth, volume, and surface area—were performed (Table 1; Figure 4, Figure 5). Specifically, the anteroposterior and mediolateral widths of the removal site entrance, the depth from the entrance surface to the bottom of the removal site, the volume,

and the total surface area of the removal site were measured (Table 1). The difference in dimensional measurements between T1 and T2 (ΔT1-T2) indicated changes in the removal site dimensions after the healing period. The healing ratio of the removal site was defined by the volume healing ratio (VHR) and the total surface area healing ratio (TSAHR), which represent the percentage of recovered bone at the palatal removal sites between T1 and T2 (Table 1). A higher healing ratio indicates more substantial palatal bone healing.

$$VHR\ (\%) = \left(1 - \frac{Volume\ of\ T2\ palatal\ removal\ site}{Volume\ of\ T1\ palatal\ removal\ site}\right) x\ 100$$

$$TSAHR\ (\%) = \left(1 - \frac{Total\ surface\ area\ of\ T2\ palatal\ removal\ site}{Total\ surface\ area\ of\ T1\ palatal\ removal\ site}\right) x\ 100$$

3. Statistical analysis

The normality of the data was verified by using Kolmogorov-Smirnov test. To compare the mean values between T1 and T2, paired t-test or Wilcoxon signed rank test were performed. Independent t-test or Mann-Whitney U-test were used to compare the changes from T1 to T2 between anterior and posterior palatal removal sites. Point-biserial correlation, Spearman's correlation, or Kendall's tau correlation tests were performed to analyze the relationships between the healing ratio of removal site and the demographic features of patients and characteristics of the miniscrews, depending on the distributional properties of the data.

Statistical analyses were performed using IBM SPSS Statistics for Windows (version 28.0; IBM Corp, Armonk, NY). A 95% confidence level ($P < 0.05$) was considered statistically significant. To evaluate the intra-examiner reliability, all measurements were repeated after a 2-week interval for 20% of the samples randomly selected by a single investigator. The intraclass correlation coefficient was over 0.80, indicating good reliability for the measurements.

Table 1. Description of measurement factors

	Measurements	Definition
Demographic features of patients	Age at T2 (years)	Age of patient at T2 (more than 6 months after miniscrew removal)
	Sex	Male/ Female
	Duration between T1-T2 (months)	Duration of time between the end of the consolidation phase before miniscrew removal (T1) and more than 6 months after miniscrew removal (T2)
	MARPE expansion width (mm)	Total amount of MARPE expansion calculated by the number of activations noted in the record
Charactetistics of miniscrew	Diameter (mm)	Diameter of the miniscrew
	Length (mm)	Length of the miniscrew
	Cortical anchorage	Number of penetrated cortical bone layer created by the miniscrew (Mono-cortical, bicortical)
	Inclination of miniscrew axis in mediolateral direction (°)	The angle measured by connecting the axis of the miniscrew to the perpendicular line of the palatal plane in mediolateral direction
	Distance to the midpalatal suture (mm)	Perpendicular distance from the center of miniscrew to the hemi-section of the MPS after expansion
	Palatal bone thickness (mm)	Palatal bone thickness at the miniscrew insertion site at T1
Measurements of the palatal removal site	Width_AP (mm)	Anteroposterior width of the removal site entrance
	Wdith_ML (mm)	Mediolateral width of the removal site entrance
	Depth (mm)	The depth from the entrance surface to the bottom of the removal site
	Volume (mm^3)	Volume of the enclosed palatal removal site
	VHR (%)	The percentage of recovered bone volume at the palatal removal sites between T1 and T2
	Total surface area (mm^2)	Total surface area of the enclosed palatal removal site
	TSAHR (%)	The percentage of recovered bone surface at the palatal removal sites between T1 and T2

III. RESULTS

1. Demographic features

This study enrolled 38 patients, including 18 men and 20 women, with a mean age at T2 of 24.7 ± 4.2 years. A total of 152 removal sites (76 anterior and 76 posterior sites) were investigated. Table 2 displays the demographic characteristics of the patients. The mean number of MARPE turns was 29.5 ± 6.1, and the mean MARPE expansion width was 5.9 ± 1.2 mm.

Table 2. Demographic features of the patients

	Patients (n = 38)	
Age at T2 (years)	24.7 ± 4.2	
Sex	Male 18 (47.4%)	Female 20 (52.6%)
Duration between T1-T2 (months)	12.0 ± 3.7	
MARPE expansion width (mm)	5.9 ± 1.2	

Data are presented as mean ± standard deviation or number (percentage).
T1, CBCT taken at the end of the consolidation phase, just before miniscrew removal; T2, CBCT taken over 6 months after miniscrew removal

Table 3 shows the miniscrew characteristics. The diameter, length, type of cortical anchorage, distance from the miniscrew to the MPS, and the PBT at the insertion site showed a statistically significant difference between the anterior and posterior miniscrews ($P < 0.001$). Miniscrews with a 1.8-mm diameter and 7-mm length were the most prevalent for both anterior and posterior miniscrews. Most anterior miniscrew had mono-cortical anchorage, while posterior miniscrews more commonly exhibited bicortical anchorage than

mono-cortical anchorage (P < 0.001). There was no statistically significant difference in the inclination of the miniscrew axis in the mediolateral direction between anterior and posterior miniscrews (P = 0.101). The distance from the posterior miniscrews to the MPS was greater than that of the anterior miniscrews (P < 0.001). In addition, the PBT at the miniscrew placement site was greater for anterior miniscrews than that for posterior ones (P < 0.001).

Table 3. Demographic features of the miniscrews

Measurements		**Anterior (n = 76)**	**Posterior (n = 76)**	**P-value**
Diameter ‡ **(mm)**	1.5	10 (13.2%)	10 (13.2%)	1.000
	1.8	58 (76.3%)	58 (76.3%)	
	2.0	8 (10.5%)	8 (10.5%)	
Length ‡ **(mm)**	6	0 (0.0%)	6 (7.9%)	< 0.001***
	7	26 (34.2%)	50 (65.8%)	
	8	10 (13.2%)	2 (2.6%)	
	9	18 (23.7%)	6 (7.9%)	
	10	4 (5.3%)	0 (0.0%)	
	11	8 (10.5%)	12 (15.8%)	
	13	10 (13.2%)	0 (0.0%)	
Cortical anchorage ‡	Monocortical	74 (97.4%)	27 (35.5%)	< 0.001***
	Bicortical	2 (2.6%)	49 (64.5%)	
Inclination of miniscrew axis in mediolateral direction† **(°)**		14.0 ± 10.2	11.7 ± 7.4	0.101
Distance to the midpalatal suture† **(mm)**		4.6 ± 1.2	3.0 ± 0.9	< 0.001***
Palatal bone thickness† **(mm)**		10.1 ± 2.1	3.8 ± 1.1	< 0.001***

Data are presented as number or mean ± standard deviation

‡ Chi-square tests were performed.

† Independent t-tests were performed to compare the anterior and posterior miniscrews.

*** $P < 0.001$

2. Healing of the palatal removal sites after removal of MARPE

The anteroposterior and mediolateral widths of the entrance, depth, volume, and total surface area of the palatal removal sites reduced significantly from T1 to T2 in both anterior and posterior removal sies ($P < 0.001$). Palatal removal sites showed VHR of 92.5 ± 9.0% and TSAHR of 82.9 ± 9.8%. The changes in the anterior palatal removal sites were greater than those in the posterior removal sites along with higher healing ratio of anterior removal sites than posterior ones ($P < 0.01$, Table 4, Figures 7 and 8). Regarding the type of cortical anchorage, the healing ratio of the palatal removal sites with mono-cortical anchorage was significantly greater than that with bicortical anchorage ($P < 0.001$, Table 5). No statistical significance in the dimensional, volumetric, and total surface changes as well as in the healing ratio between palatal removal site on left and right side was found ($P > 0.05$).

3. Relationship between the healing ratio of the palatal removal sites and demographic features of the patient and characteristics of miniscrew

The healing ratio of the posterior palatal removal sites showed significant relationship with most of the variables ($P < 0.05$), while those of the anterior removal sites did not show significant relationship with any demographic features of patients and

miniscrew characteristics ($P > 0.05$, Table 6). VHR of the posterior palatal removal sites showed positive correlations with the duration ($r = 0.239$; $P = 0.037$) and the PBT ($r = 0.491$, $P < 0.001$); but negative correlations with age at T2 ($r = -0.350$; $P = 0.002$), MARPE expansion width ($r = -0.265$; $P = 0.021$), distance from miniscrew to MPS ($r = -0.514$; $P < 0.001$), and type of cortical anchorage ($r = -0.391$, $P < 0.001$). Similarly, TSAHR of the posterior palatal removal sites showed positive correlations with the duration ($r = 0.308$; $P = 0.007$) and the PBT ($r = 0.527$; $P < 0.001$); but negative correlation with age at T2 ($r = -0.353$; $P = 0.002$), MARPE expansion width ($r = -0.272$; $P = 0.018$), distance from miniscrew to MPS ($r = -0.543$; $P < 0.001$), and type of cortical anchorage ($r = -0.363$; $P < 0.001$) (Table 7).

The linear regression models led to the equations as follows (Figure 9):

VHR = 1.030 – (0.006 x age at T2) + 0.005 x (time duration) – (0.019 x MARPE expansion width) – (0.030 x distance to MPS) + (0.033 x PBT)

TSAHR = 0.896 – (0.007 x age at T2) + (0.007 x time duration) – (0.017 x MARPE expansion witdth) – (0.035 x distance to MPS) + (0.039 x PBT).

Table 4. Dimensional measurement, volume, total surface, and healing ratio of the palatal removal sites at T1 and T2

Measure_ments	Anterior (n = 76)				Posterior (n = 76)				Sig. †
	T1§	T2§	ΔT1-T2†	P-value§	T1§	T2§	ΔT1-T2†	P-value§	
Width_AP (mm)	2.3 ± 0.4	1.5 ± 0.3	0.8 ± 0.4	< 0.001***	2.4 ± 0.6	1.7 ± 0.4	0.7 ± 0.5	< 0.001***	0.003**
Width_ML (mm)	2.3 ± 0.4	1.4 ± 0.3	0.9 ± 0.4	< 0.001***	2.2 ± 0.3	1.6 ± 0.3	0.6 ± 0.3	< 0.001***	< 0.001***
Depth (mm)	5.2 ± 1.3	0.3 ± 0.1	5.0 ± 1.3	< 0.001***	3.3 ± 0.8	0.7 ± 0.4	2.6 ± 0.9	< 0.001***	< 0.001***
Volume (mm^3)	14.9 ± 5.4	0.3 ± 0.2	14.7 ± 5.3	< 0.001***	8.3 ± 2.7	1.1 ± 0.9	7.2 ± 2.5	< 0.001***	< 0.001***
VHR (%)			98.3 ± 1.1				86.6 ± 9.7		< 0.001***
Total surface area (mm^2)	38.5 ± 9.8	4.3 ± 2.0	34.3 ± 8.9	< 0.001***	26.5 ± 6.8	6.1 ± 3.3	20.4 ± 5.9	< 0.001***	< 0.001***
TSAHR (%)			88.9 ± 4.3				77.0 ± 10.2		< 0.001***

Data are presented as mean ± standard deviation.

† Mann-Whitney U test or independent t-test were performed to compare the mean value of ΔT1-T2 between anterior palatal defects and posterior palatal removal sites.

§ Wilcoxon signed rank test or paired t-test were performed to compare the mean value between T1 and T2

T1, CBCT taking within 1 month after the consolidation phase; T2, CBCT taking over 6 months after the removal of miniscrews

Width_AP, width of the removal site entrance in anteroposterior direction; Width_ML, width of the entrance in mediolateral direction; Depth, depth of the palatal removal sites. VHR, Volume healing ratio of the palatal removal site;

$$\text{VHR (\%)} = \left(1 - \frac{\text{Volume of T2 palatal removal site}}{\text{Volume of T1 palatal removal site}}\right) \text{x } 100$$

TSAHR, Total surface area healing ratio of the palatal removal site;

$$\text{TSAHR (\%)} = \left(1 - \frac{\text{Total surface area of T2 palatal removal site}}{\text{Total surface area of T1 palatal removal site}}\right) \text{x } 100$$

**P < 0.01; ** P < 0.001

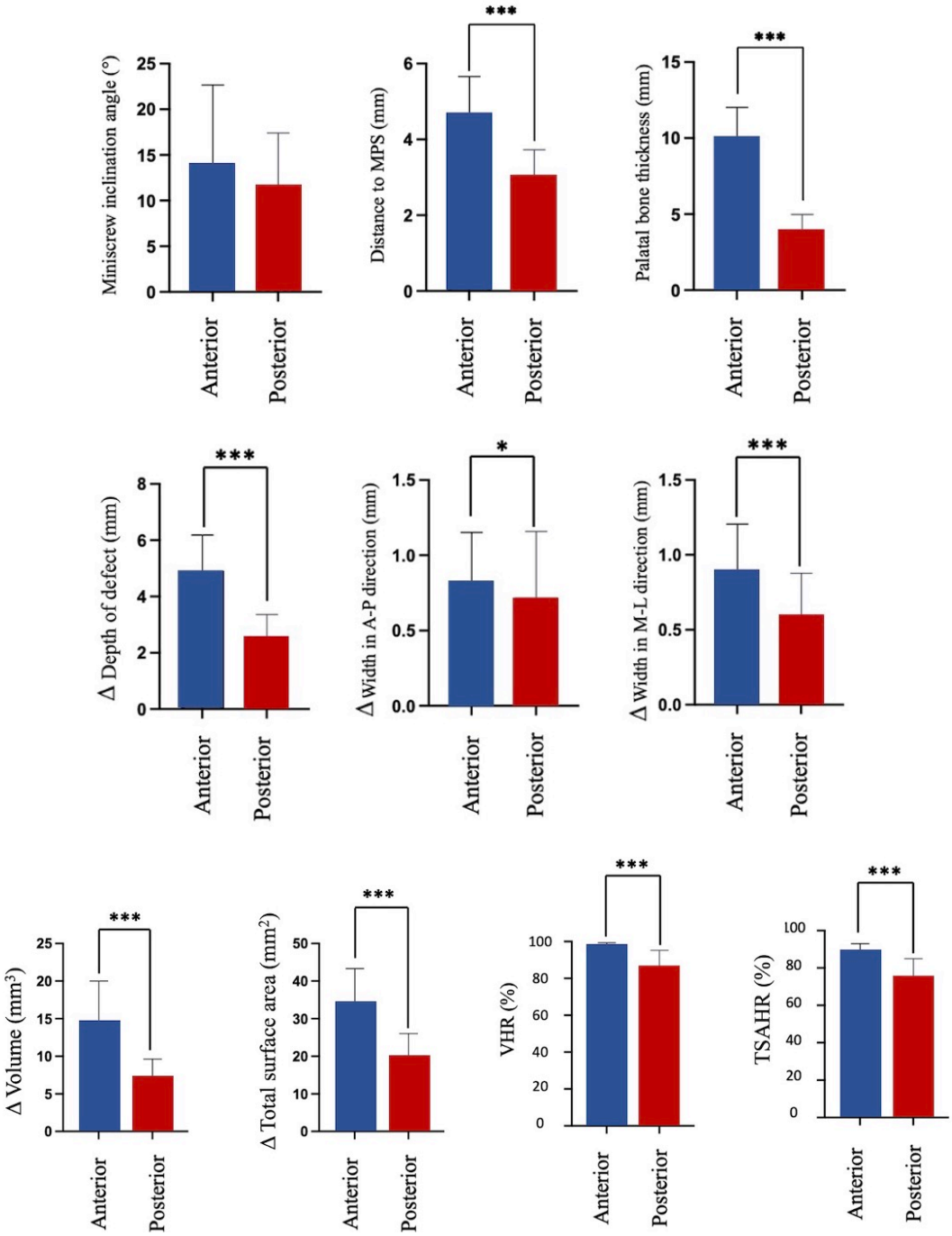

Figure 7. Comparison of miniscrew position, removal site dimensions, and healing after miniscrew removal between anterior and posterior palatal removal sites. The miniscrew inclination angle in the mediolateral (M-L) direction, distance from the miniscrew to the midpalatal suture (MPS), and palatal bone thickness at the miniscrew insertion site were investigated at T1. Changes in dimensional measurements, including widths, depth, volume, and total surface area of the removal site were performed between T1 and T2. A-P, anteroposterior;

VHR, Volume healing ratio of the palatal removal site;

$$\text{VHR}\ (\%) = \left(1 - \frac{\text{Volume of T2 palatal removal site}}{\text{Volume of T1 palatal removal site}}\right) \text{x } 100$$

TSAHR, Total surface area healing ratio of the palatal removal site;

$$\text{TSAHR}\ (\%) = \left(1 - \frac{\text{Total surface area of T2 palatal removal site}}{\text{Total surface area of T1 palatal removal site}}\right) \text{x } 100$$

Table 5. Healing ratio of the palatal removal sites depending on the type of cortical anchorage

	Mono-cortical anchorage (n = 101)	**Bicortical anchorage** (n = 51)	**P-value**
VHR (%)	96.5 ± 4.6	84.4 ± 10.2	< 0.001***
TSAHR (%)	87.0 ± 6.0	74.8 ± 10.9	< 0.001***

Independent t-tests were performed; Data are presented as mean ± standard deviation

VHR, Volume healing ratio of the palatal removal site;

$$\text{VHR (\%)} = \left(1 - \frac{\text{Volume of T2 palatal removal site}}{\text{Volume of T1 palatal removal site}}\right) \text{x } 100$$

TSAHR, Total surface area healing ratio of the palatal removal site;

$$\text{TSAHR (\%)} = \left(1 - \frac{\text{Total surface area of T2 palatal removal site}}{\text{Total surface area of T1 palatal removal site}}\right) \text{x } 100$$

Table 6. Correlation between healing ratio of the palatal removal sites and demographic features of the patient and characteristics of the miniscrew.

	Anterior palatal removal site				Posterior palatal removal site			
	VHR (%)		TSAHR (%)		VHR (%)		TSAHR (%)	
	r	P-value	r	P-value	r	P-value	r	P-value
Age at T2[†] (years)	0.009	0.936	-0.051	0.662	-0.350	0.002**	-0.353	0.002**
Sex[‡]	-0.098	0.401	-0.120	0.303	-0.039	0.738	-0.088	0.448
Duration[†] (months)	-0.131	0.259	0.039	0.739	0.239	0.037*	0.308	0.007**
MARPE expansion width[†] (mm)	0.161	0.166	0.109	0.349	-0.265	0.021*	-0.272	0.018*
Diameter[§] (mm)	-0.040	0.663	-0.136	0.140	0.057	0.537	0.067	0.468
Length[§] (mm)	-0.002	0.985	-0.013	0.875	-0.005	0.957	-0.043	0.631
Inclination[†] (°)	-0.148	0.200	-0.159	0.171	-0.127	0.274	-0.078	0.504
Distance to MPS[†] (mm)	0.114	0.328	0.087	0.452	-0.514	< 0.001***	-0.543	< 0.001***
PBT[†] (mm)	0.070	0.547	0.104	0.371	0.491	< 0.001***	0.527	< 0.001***
Cortical anchorage[‡]	-0.003	0.977	-0.005	0.969	-0.391	< 0.001***	-0.363	0.001**

[‡] Point-biserial correlation test was performed, [†] Spearman correlation test was performed, [§] Kendall's tau correlation test was performed

Duration, the time between T1 and T2; MARPE expansion, amount of miniscrew-assisted rapid palatal expander (MARPE) expansion; diameter, diameter of the miniscrew; length,

length of the miniscrew; inclination, inclination of miniscrew axis in the mediolateral direction; distance to MPS, distance from the miniscrew to the midpalatal suture; PBT, palatal bone thickness; T1, CBCT taking within 1 month after the consolidation phase; T2, CBCT taking over 6 months after the removal of miniscrews; r, correlation coefficient

VHR, Volume healing ratio of the palatal removal site;

$$\text{VHR}\ (\%) = \left(1 - \frac{\text{Volume of T2 palatal removal site}}{\text{Volume of T1 palatal removal site}}\right) \text{x } 100$$

TSAHR, Total surface area healing ratio of the palatal removal site;

$$\text{TSAHR}\ (\%) = \left(1 - \frac{\text{Total surface area of T2 palatal removal site}}{\text{Total surface area of T1 palatal removal site}}\right) \text{x } 100$$

Table 7. Summary of multiple regression analysis for variables predicting healing ratio of posterior palatal removal sites

Dependent variable	Independent variable	Unstandardized coefficients		Adjusted R^2	95% Confidence interval for B		P value
		B	SE		Lower bound	Upper bound	
VHR (%)	(Constant)	1.030	0.084	0.567	0.863	1.197	< 0.001***
	Age at T2 (years)	-0.006	0.002		-0.010	-0.002	0.002**
	Duration (months)	0.005	0.002		0.001	0.009	0.007**
	MARPE expansion (mm)	-0.019	0.006		-0.032	-0.006	0.005**
	Distance to MPS (mm)	-0.030	0.009		-0.048	-0.012	0.002**
	PBT (mm)	0.033	0.008		0.016	0.050	< 0.001**
	Cortical anchorage	-0.004	0.019		-0.042	0.035	0.853
TSAHR (%)	(Constant)	0.896	0.082	0.626	0.733	1.059	< 0.001***
	Age (years)	-0.007	0.002		-0.011	-0.003	< 0.001***
	Duration (months)	0.007	0.002		0.003	0.010	< 0.001***
	MARPE expansion (mm)	-0.017	0.006		-0.030	-0.005	0.008**
	Distance to MPS (mm)	-0.035	0.009		-0.052	-0.017	< 0.001***
	PBT (mm)	0.039	0.008		0.023	0.056	< 0.001**
	Cortical anchorage	0.011	0.019		-0.027	0.048	0.571

B, unstandardized regression coefficient; SE, standard error; T2, CBCT taking over 6 months after the removal of miniscrews; Duration, duration of time between T1 and T2; MARPE expansion, amount of MARPE expansion width; Distance to MPS, distance from the miniscrew to midpalatal suture; PBT, palatal bone thickness

VHR, Volume healing ratio of the palatal removal site;

$$\text{VHR (\%)} = \left(1 - \frac{\text{Volume of T2 palatal removal site}}{\text{Volume of T1 palatal removal site}}\right) \text{x } 100$$

TSAHR, Total surface area healing ratio of the palatal removal site;

$$\text{TSAHR (\%)} = \left(1 - \frac{\text{Total surface area of T2 palatal removal site}}{\text{Total surface area of T1 palatal removal site}}\right) \text{x } 100$$

* $P < 0.05$; ** $P < 0.01$; *** $P < 0.001$

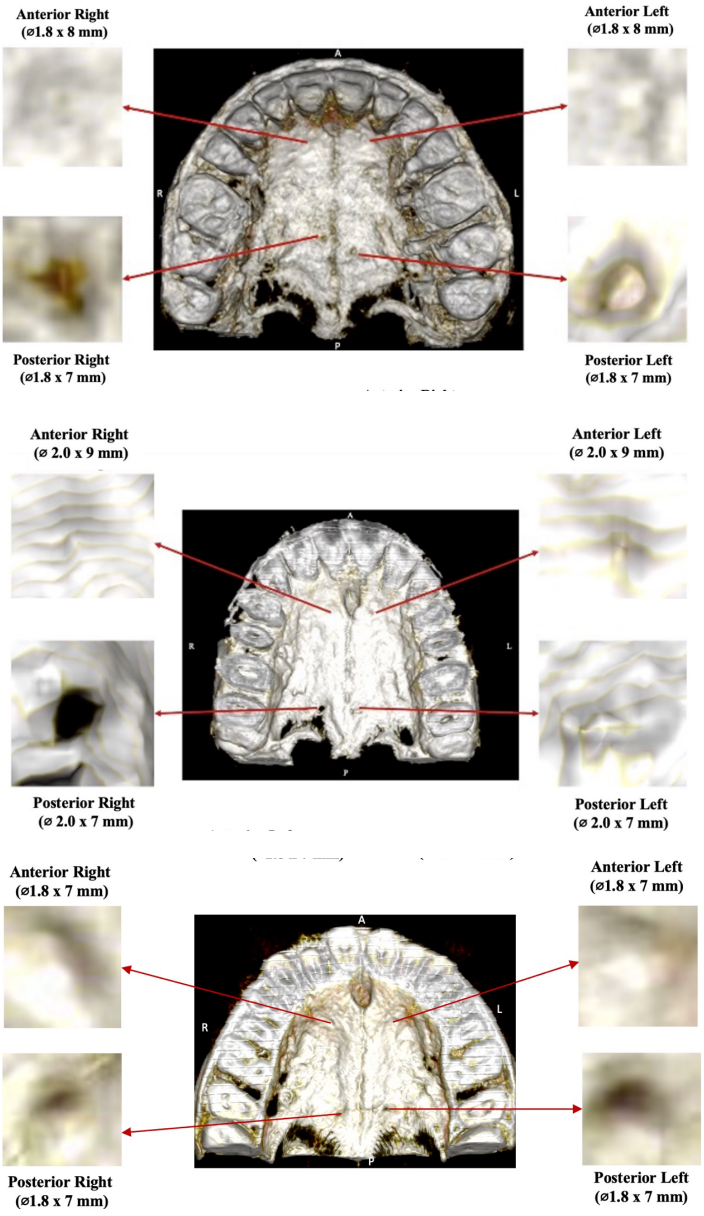

Figure 8. Palatal bony surface at T2 showing bone healing after miniscrew removal.

A, anterior; P, posterior; R, right; L, left; T2, CBCT taken over 6 months after miniscrew removal; ⌀, diameter of the miniscrew.

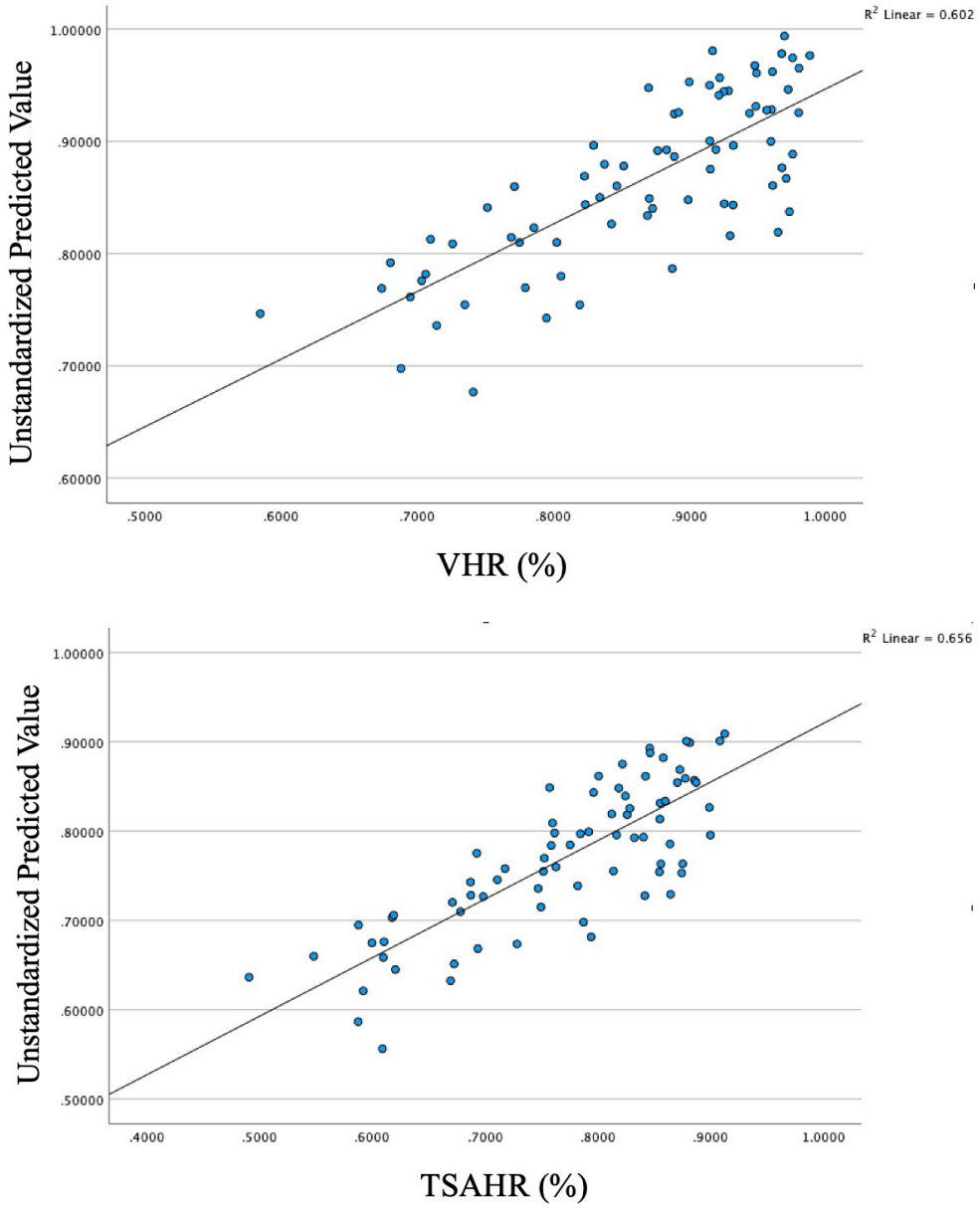

Figure 9. Scatter plot of the multiple regression analysis for variables predicting the healing ratio of posterior palatal removal sites

IV. DISCUSSION

This study examines the healing of palatal removal sites following the miniscrews removal in patients with maxillary constriction treated through orthopedic expansion—a subject that has been underexplored in the literature. In the present study, palatal removal sites showed a VHR of 92.5% and a TSAHR of 82.9%, indicating significant healing after miniscrew removal and leading to the rejection of the null hypothesis. Anterior removal sites demonstrated a 98.3% volume healing ratio, while posterior removal sites showed an 86.6% healing ratio. Removal sites with mono-cortical anchorage exhibited a 96.5% healing ratio, significantly higher than the 84.4% observed in those with bicortical anchorage. These findings suggest that palatal removal sites nearly recover their original volume following MARPE treatment. However, the potential formation of a crater on the palatal surface after posterior miniscrew removal warrants careful consideration during treatment planning and procedural steps.

After miniscrews removal, the dimensions of the palatal removal sites formed by miniscrew decreased noticeably. The VHR of palatal removal sites after maxillary expansion was 92.5%, and the TSAHR was 82.9%, indicating significant recovery of palatal bone at the removal site. Notwithstanding the great amount of orthopedic expansion force in MARPE treatment as well as the concentrated maximum stress arounds the miniscrews incorporated with MARPE, the finding from the present study suggests that the palatal bone at the miniscrew removal site might have potential to recover their original integrity after enduring orthopedic expansion force (Walter et al., 2023; MacGinnis et al., 2014; Reynders et al., 2009; Seong et al., 2018). Nevertheless, the finding from the present study suggests that the palatal bone at the miniscrew removal site might have potential to

recover their original integrity after enduring orthopedic expansion force. Significant recovery has also been observed in the alveolar bone of dog models following the removal of orthodontic miniscrews, despite a transient defect extending through the gingival soft tissue, cortical bone, and cancellous bone (Kim et al., 2019).

The healing of anterior removal sites (VHR of 98.3% and TSAHR of 86.6%) was significantly greater than that of posterior removal sites (VHR of 88.9% and TSAHR of 77 %). This difference may be attributed to variations in palatal bone thickness and bone density, and vascularization. Palatal bone thickness and density gradually decrease toward the posterior region, indicating that the anterior palate is both thicker and denser than the posterior palate (Kyung et al., 2004; Chang et al., 2021; Suteerapongpun et al., 2018; Moon et al., 2010). However, since cortical bone thickness does not significantly vary across different palatal regions, the thinner and less dense cancellous bone in the posterior palate might contribute to the lower healing ratio (Chang et al., 2021). Additionally, anterior palatal removal sites are located near the major branches of the greater palatine artery and its anastomosis with the nasopalatine artery, while posterior removal sites are located in the mid-palate, closer to the minor branches of the greater palatine artery, which have a less robust blood supply (Shahbazi et al., 2019; Kim et al., 2014).

The significantly lower healing ratio of palatal removal sites with bicortical anchorage compared to those with mono-cortical anchorage suggests that the double penetration to cortical bone layers seems to reduce the healing capacity. When mechanical stress occurs, resorption begins in the cortical bone and continues until the entire damaged area is resorbed, without affecting the cancellous bone, which has a rich defense and recovery mechanism (Davies, 2003; Pittenger et al., 1999). In cortical bone, the limited availability of local mesenchymal cells attributes to the longer duration required for bone formation compared to cancellous bone. (Sandberg et al., 2016; Kumagai et al., 2008; Liu et al., 2011; Neagu et al., 2016). Conversely, cancellous bone, which is abundant in mesenchymal

cells—particularly endosteal mesenchymal cells—exhibits high regenerative potential (Siclari et al., 2013). Additionally, a penetration of double layers of cortical bone can conduct to the risk of perforation into the maxillary sinus and may create an oral-sinus communication as well as sinus infection that generate inflammation and pain (Copello et al., 2021). The association between inflammatory conditions and impaired bone regeneration was explained in previous litterature (Newman et al., 2021). Therefore, although miniscrews with bicortical anchorage provide greater stability, less miniscrew deformation, and more parallel expansion, they require clinicians' attention due to the potential perforation into the nasal cavity and insufficient healing after the removal (Lee et al., 2017; Bourassa et al., 2018).

Variations in the healing ratio of posterior palatal removal sites were observed depending on patient demographics and miniscrew characteristics. A decrease in T2 age and an increase in the duration between T1 and T2 were significantly associated with a higher healing ratio, suggesting that younger patients with a longer healing period experienced better outcomes, as previously reported (Naveda et al., 2022; Gibon et al., 2016). Positive correlation of the healing ratio with PBT but negative correlations with the distance from miniscrew to MPS as well as cortical anchorage indicated that greater healing occurred in patients with thicker palatal bone, miniscrews placed closer to the MPS, and mono-cortical anchorage. The bone thickness at the damaged site can influence the process of healing (Li et al., 2023). The findings of the present study suggest that removal sites closer to the MPS, which were confirmed to have greater PBT, showed a higher healing ratio compared to those located further away from the MPS (Kang et al.; 2007; Negrisoli et al., 2022). Additionally, the negative correlation between the healing ratio and MARPE expansion width suggests that smaller maxillary expansion width leads to better bone healing. No significant correlations were observed for anterior palatal removal sites, likely due to the consistently high healing ratio in this region.

This study had some limitations. While histomorphometric analysis would have provided a more accurate assessment of palatal wound healing after miniscrew removal than CBCT evaluation, the use of CBCT was the best available option given that the study involved living patients. Another limitation was the inability to precisely replicate the palatal surface as it appeared at T1, due to the presence of the miniscrew. Furthermore, because this study was retrospective and clinical in nature, variables such as age at T2, healing duration, miniscrew dimensions, skill for miniscrew installation, MARPE design, amount of expansion, and consolidation time were not controlled. The short-term observation period was also a limitation. Even though well trained one observer performed the image analysis, there might be innate error due to the small size of ROI. Despite these limitations, the findings offer scientific evidence and valuable insights into the healing capacity of palatal bone after miniscrew removal under orthopedic expansion. Almost complete healing of the palatal bone can be expected, particularly in anterior palate; however, greater attentions should be given to posterior miniscrews with bicortical anchorage. Further research with larger sample sizes, investigating the short-term as well as long-term healing of palatal bone after miniscrew removal under orthodontic and orthopedic force, would further enhance our understanding of palatal bone healing.

V. CONCLUSION

- The null hypothesis that there is no healing of the palatal removal sites after miniscrew removal was rejected.
- Significant palatal bone healing was observed in average 12 months after miniscrew removal in patients treated with MARPE, with a VHR of 92.5%, and TSAHR of 82.9%. Although small defects may remain at the removal site, they can be considered clinically insignificant.
- The healing ratio was significantly higher for anterior removal sites compared to posterior removal sites and for mono-cortical anchorage compared to bicortical anchorage.
- Better palatal bone healing after MARPE removal was associated with younger age, longer healing duration, smaller maxillary expansion width, closer proximity to the midpalatal suture, thicker palatal bone, and mono-cortical anchorage.

REFERENCES

Bazina, M., Cevidanes, L., Ruellas, A., Valiathan, M., Quereshy, F., Syed, A., ... & Palomo, J. M. (2018). Precision and reliability of Dolphin 3-dimensional voxel-based superimposition. *American Journal of Orthodontics and Dentofacial Orthopedics*, *153*(4), 599-606.

Bourassa, C., Hosein, Y. K., Pollmann, S. I., Galil, K., Bohay, R. N., Holdsworth, D. W., & Tassi, A. (2018). In-vitro comparison of different palatal sites for orthodontic miniscrew insertion: Effect of bone quality and quantity on primary stability. *American Journal of Orthodontics and Dentofacial Orthopedics*, *154*(6), 809-819.

Brunelle JA, Bhat M, Lipton JA (1996). Prevalence and distribution of selected occlusal characteristics in the US population, 1988-1991. *Journal of Dental Research,* 75 Spec No:706-713.

Cevidanes, L. H., Heymann, G., Cornelis, M. A., DeClerck, H. J., & Tulloch, J. C. (2009). Superimposition of 3-dimensional cone-beam computed tomography models of growing patients. *American Journal of Orthodontics and Dentofacial Orthopedics*, *136*(1), 94-99.

Chang, C. J., Lin, W. C., Chen, M. Y., & Chang, H. C. (2021). Evaluation of total bone and cortical bone thickness of the palate for temporary anchorage device insertion. *Journal of Dental Sciences*, *16*(2), 636-642.

Charton, J., Baek, S., Kim, Y. (2020). Mesh repairing using topology graphs. *Journal of Computational Design and Engineering*, 8(1):251-267.

Choi, Y. J., Lee, D. W., Kim, K. H., & Chung, C. J. (2015). Scar formation and revision after the removal of orthodontic miniscrews. *The Korean Journal of Orthodontics*, *45*(3), 146-150.

Colebank, M. J., Paun, L. M., Qureshi, M. U. (2019). Influence of image segmentation on one-dimensional fluid dynamics predictions in the mouse pulmonary arteries. *Journal of the Royal Society Interface*, 16(159):20190284.

Copello, F. M., Brunetto, D. P., Elias. C. N. (2021). Miniscrew-assisted rapid palatal expansion (MARPE): how to achieve greater stability. In vitro study. *Dental Press Journal of Orthodontics*, 26(1):e211967.

Davies, J. E. (2003). Understanding peri-implant endosseous healing. *Journal of dental education*, *67*(8), 932-949.

de Freitas, B. N., Mendonça, L. M., Cruvinel, P. B., de Lacerda, T. J., Leite, F. G. J., Oliveira-Santos, C., & Tirapelli, C. (2023). Comparison of intraoral scanning and CBCT to generate digital and 3D-printed casts by fused deposition modeling and digital light processing. *Journal of dentistry*, *128*, 104387.

Fäh, R., & Schätzle, M. (2014). Complications and adverse patient reactions associated with the surgical insertion and removal of palatal implants: a retrospective study. *Clinical Oral Implants Research*, *25*(6), 653-658.

Friedli, L., Kloukos D., Kanavakis, G., Halazonetis, D., Gkantidis, N. (2020). The effect of threshold level on bone segmentation of cranial base structures from CT and CBCT images. *Scientific Reports*, 10(1):7361

Gibon, E., Lu, L., & Goodman, S. B. (2016). Aging, inflammation, stem cells, and bone healing. *Stem cell research & therapy*, *7*, 1-7.

Gomes, A. F., Brasil D,. M., Silva, A. I. V. (2020). Accuracy of ITK-SNAP software for 3D analysis of a non-regular topography structure. *Oral Radiology*, 36(2):183-89.

Haas, A. J. (1961). Rapid expansion of the maxillary dental arch and nasal cavity by opening the midpalatal suture. *The Angle Orthodontist*, *31*(2), 73-90.

Jeon, J. Y., Choi, S. H., Chung, C. J., & Lee, K. J. (2022). The success and effectiveness of miniscrew-assisted rapid palatal expansion are age-and sex-dependent. *Clinical oral investigations*, *26*(3), 2993-3003.

Jung, S. A., Choi, Y. J., Lee, D. W., Kim, K. H., & Chung, C. J. (2015). Cross-sectional evaluation of the prevalence and factors associated with soft tissue scarring after the removal of miniscrews. *The Angle Orthodontist*, *85*(3), 420-426.

Kang, S., Lee, S. J., Ahn, S. J., Heo, M. S., & Kim, T. W. (2007). Bone thickness of the palate for orthodontic mini-implant anchorage in adults. *American Journal of Orthodontics and Dentofacial Orthopedics*, *131*(4), S74-S81.

Kim, D. H., Won, S. Y., Bae, J. H., Jung, U. W., Park, D. S., Kim, H. J., & Hu, K. S. (2014). Topography of the greater palatine artery and the palatal vault for various types of periodontal plastic surgery. *Clinical Anatomy*, *27*(4), 578-584.

Kim, S. J., Ha, Y. D., Kim, E., Jang, W., Hwang, S., Nguyen, T., ... & Chung, C. J. (2019). Dynamics of alveolar bone healing after the removal of orthodontic temporary anchorage devices. *Journal of Periodontal Research*, *54*(4), 388-395.

Kravitz, N. D., & Kusnoto, B. (2007). Risks and complications of orthodontic miniscrews. *American Journal of Orthodontics and Dentofacial Orthopedics*, *131*(4), S43-S51.

Kumagai, K., Vasanji, A., Drazba, J. A., Butler, R. S., & Muschler, G. F. (2008). Circulating cells with osteogenic potential are physiologically mobilized into the fracture healing site in the parabiotic mice model. *Journal of orthopaedic research*, *26*(2), 165-175.

Kyung, S. H. (2004). A study on the bone thickness of midpalatal suture area for miniscrew insertion. *Korean Journal of Orthodontics*, 63-70.

Lee, J. M., Choi, S. H., Choi, Y. J., Lee, K. J., & Yu, H. S. (2023). Evaluation of miniscrew-assisted rapid palatal expansion success by comparing width of circummaxillary

sutures before expansion in adult male patients. *The Angle Orthodontist*, *93*(2), 176-184.

Lee, K. J., Park, Y. C., Park, J. Y., & Hwang, W. S. (2010). Miniscrew-assisted nonsurgical palatal expansion before orthognathic surgery for a patient with severe mandibular prognathism. *American Journal of Orthodontics and Dentofacial Orthopedics*, *137*(6), 830-839.

Lee, R.J., Pham, J., Choy, M. (2014). Monitoring of typodont root movement via crown superimposition of single cone-beam computed tomography and consecutive intraoral scans. *American Journal of Orthodontics and Dentofacial Orthopedics*, 145(3):399-409.

Lee, R. J., Moon, W., & Hong, C. (2017). Effects of monocortical and bicortical mini-implant anchorage on bone-borne palatal expansion using finite element analysis. *American Journal of Orthodontics and Dentofacial Orthopedics*, *151*(5), 887-897.

Li, S. Z. (1995). Adaptive sampling and mesh generation. *Computer-Aided Design*, 27(3):235-240.

Li, Y., Yang, Z., Tong, L., Yang, J., Wang, J., & Wen, Y. (2023). Wall thickness analysis method for judging the degree of lower extremity long bone healing. *Scientific Reports*, *13*(1), 20650.

Liu, R., Birke, O., Morse, A., Peacock, L., Mikulec, K., Little, D. G., & Schindeler, A. (2011). Myogenic progenitors contribute to open but not closed fracture repair. *BMC musculoskeletal disorders*, *12*, 1-9.

MacGinnis, M., Chu, H., Youssef, G., Wu, K. W., Machado, A. W., & Moon, W. (2014). The effects of micro-implant assisted rapid palatal expansion (MARPE) on the nasomaxillary complex—a finite element method (FEM) analysis. *Progress in orthodontics*, *15*, 1-15.

Moon, S. H., Park, S. H., Lim, W. H., & Chun, Y. S. (2010). Palatal bone density in adult subjects: implications for mini-implant placement. *The Angle Orthodontist*, *80*(1), 137-144.

Naveda, R., Dos Santos, A. M., Seminario, M. P., Miranda, F., Janson, G., & Garib, D. (2022). Midpalatal suture bone repair after miniscrew-assisted rapid palatal expansion in adults. *Progress in Orthodontics*, *23*(1), 35.

Nagarajappa, A. K., Dwivedi N., Tiwari R. (2015) Artifacts: The downturn of CBCT image. *Journal of International Society of Preventive and Community Dentistry*; 5(6):440-445.

Neagu, T. P., Ţigliş, M., Cocoloş, I., & Jecan, C. R. (2016). The relationship between periosteum and fracture healing. *Romanian Journal of Morphology and Embryology*, *57*(4), 1215-1220.

Negrisoli, S., Angelieri, F., Gonçalves, J. R., da Silva, H. D. P., Maltagliati, L. Á., & Nahás-Scocate, A. C. R. (2022). Assessment of the bone thickness of the palate on cone-beam computed tomography for placement of miniscrew-assisted rapid palatal expansion appliances. *American Journal of Orthodontics and Dentofacial Orthopedics*, *161*(6), 849-857.

Newman, H., Shih, Y. V., Varghese, S. (2021). Resolution of inflammation in bone regeneration: From understandings to therapeutic applications. *Biomaterials*, 277:121114.

Pittenger, M. F., Mackay, A. M., Beck, S. C., Jaiswal, R. K., Douglas, R., Mosca, J. D., ... & Marshak, D. R. (1999). Multilineage potential of adult human mesenchymal stem cells. *Science*, *284*(5411), 143-147.

Reynders, R., Ronchi, L., & Bipat, S. (2009). Mini-implants in orthodontics: a systematic review of the literature. *American Journal of Orthodontics and Dentofacial Orthopedics*, *135*(5), 564-e1.

Sandberg, O. H., & Aspenberg, P. (2016). Inter-trabecular bone formation: a specific mechanism for healing of cancellous bone: A narrative review. *Acta orthopaedica*, *87*(5), 459-465.

Seong, E. H., Choi, S. H., Kim, H. J., Yu, H. S., Park, Y. C., & Lee, K. J. (2018). Evaluation of the effects of miniscrew incorporation in palatal expanders for young adults using finite element analysis. *The Korean Journal of Orthodontics*, *48*(2), 81-89.

Shahbazi, A., Grimm, A., Feigl, G., Gerber, G., Székely, A. D., Molnár, B., & Windisch, P. (2019). Analysis of blood supply in the hard palate and maxillary tuberosity—clinical implications for flap design and soft tissue graft harvesting (a human cadaver study). *Clinical Oral Investigations*, *23*, 1153-1160.

Siclari, V. A., Zhu, J., Akiyama, K., Liu, F., Zhang, X., Chandra, A., ... & Qin, L. (2013). Mesenchymal progenitors residing close to the bone surface are functionally distinct from those in the central bone marrow. *Bone*, *53*(2), 575-586.

Suteerapongpun, P., Wattanachai, T., Janhom, A., Tripuwabhrut, P., & Jotikasthira, D. (2018). Quantitative evaluation of palatal bone thickness in patients with normal and open vertical skeletal configurations using cone-beam computed tomography. *Imaging science in dentistry*, *48*(1), 51.

Yushkevich, P. A., Piven, J., Hazlett, H.C (2006). User-guided 3D active contour segmentation of anatomical structures: significantly improved efficiency and reliability. *Neuroimage*, 31(3):1116-1128.

Yushkevich, P. A., Pashchinskiy, A., Oguz, I. (2019) User-Guided Segmentation of Multi-modality Medical Imaging Datasets with ITK-SNAP. *Neuroinformatics*, 17(1):83-102.

Walter, A., de la Iglesia, F., Winsauer, H., Ploder, O., Wendl, B., & Puigdollers Perez, A. (2023). Evaluation of expansion forces of five pure bone-borne maxillary expander

designs anchored with orthodontic mini-implants: An in vitro study. *Journal of Orthodontics*, *50*(4), 335-343.

국문 요약

미니스크류 지지형 급속구개확장 장치 제거 후 구개 제거 부위의 치유

연세대학교 대학원 치의학과

(지도교수 최 윤 정)

Nguyen Hieu

본 연구는 MARPE 치료를 받은 환자의 미니스크류 제거 후 구개 제거 부위의 치유 과정을 CBCT 영상을 통해 평가하는 것을 목적으로 하였다. 또한, 제거 부위의 치유 비율과 미니스크류 식립 위치 간의 상관관계를 분석하고자 하였다..

본 후향적 연구는 MARPE 치료를 받은 성인 환자 38 명으로부터 수집된 152 개 제거 부위(전방 76 개, 후방 76 개)를 대상으로 하였다. 구개골 제거 부위의 치유 상태를 조사하기 위해 다음과 같은 지표가 측정되었다: 미니스크류 축 경사도,

미니스크류와 정중구개봉합(MPS) 간 거리, 구개골 두께, 전후 및 좌우 방향 너비, 제거 부위 입구에서 바닥까지의 깊이, 체적, 총 표면적. 또한, 부피 치유 비율(VHR)과 총 표면적 치유 비율(TSAHR)이 분석되었으며, 전방 및 후방 제거 부위 간, 단피질 및 양피질 고정 장치 간 치유 비율을 비교하였다. 구개골 제거 부위의 치유 비율과 환자 및 미니스크류의 인구학적· 치유율과 환자의 인구통계학적 및 임상적 요인 간 상관관계도 분석하였다.

미니스크류 제거 후 제거 부위의 크기, 체적 및 총 표면적이 유의미하게 감소하였다($P < 0.05$). 전방 제거 부위의 VHR(98.3 ± 1.1%)은 후방 제거 부위의 VHR(86.6 ± 9.7%)보다 유의미하게 높았으며($P < 0.001$), 단피질 고정 장치의 VHR(96.5 ± 4.6%)은 양피질 고정 장치의 VHR(84.4 ± 10.2%)보다 유의미하게 높았다($P < 0.001$). 후방 제거 부위의 치유 비율은 T2 시점의 나이, 치료 경과 기간, MARPE 확장 폭, MPS 까지의 거리 및 고정 장치 유형과 유의한 상관관계를 보였다($P < 0.05$).

MARPE 제거 후 구개 제거 부위는 유의미한 회복을 보였으며, 전방 및 단피질 고정 장치에서의 치유 비율이 각각 후방 및 양피질 고정 장치보다 높게 나타났다.

후방 제거 부위의 치유 비율은 환자의 다양한 인구학적 특성과 미니스크류의 특성에 의해 영향을 받을 수 있는 것으로 보인다.

핵심이 되는 말: MARPE, palatal bone, bone healing, miniscrew.